Molecular BioSystems

PAPER

View Article Online
View Journal | View Issue

Cite this: *Mol. BioSyst.*, 2014, **10**, 2914

Dynamic changes in metabolic profiles of rats subchronically exposed to mequindox†

Limiao Jiang,‡[a] Xiuju Zhao,§[a] Chongyang Huang,[a] Hehua Lei,[a] Huiru Tang[ab] and Yulan Wang*[ac]

Received 4th April 2014,
Accepted 4th August 2014

DOI: 10.1039/c4mb00218k

www.rsc.org/molecularbiosystems

Mequindox is widely used as an antibacterial veterinary drug and a feeding additive for farm animals in China. Although its toxicity has been widely studied, little is known regarding the metabolic effects of subchronic exposure to mequindox, which is vital for the health of meat producing livestock. Here, we characterized the dose- and time-dependent metabolic alterations in female Wistar rats subchronically exposed to mequindox through dietary supplementation at the level of 40, 110 and 280 mg kg^{-1} for 13 weeks, employing a NMR based metabonomics approach with supplementary information from serum clinical chemistry. We found that urinary metabolic profiles were significantly affected in all dosed groups during the supplementation period; plasma and hepatic metabolic profiles were significantly affected only in rats dosed with moderate and high levels of mequindox. We also observed a return to control levels, for the profiles of urine and liver, at all dose levels after a two weeks washout period. However, this was not the case for the metabolic profiles of plasma from rats dosed at high levels. At the molecular level, we showed that subchronic exposure to mequindox resulted in tricarboxylic acid cycle (TCA cycle) stimulation, suppression of glycolysis, and promotion of gluconeogenesis and lipid oxidation in rats. In addition, subchronic exposure to mequindox induced oxidative stress in rats. Furthermore, a disturbance of gut microbiota, manifested by alterations in the urinary excretion of hippurate, phenylacetylglycine, 3-(3-hydroxyphenyl)propionate, *p*-cresol glucuronide, methylamine, dimethylamine, and formate, was associated with mequindox exposure. The present study provided important holistic metabolic information on the effects of subchronic dosage of mequindox on rats, which is useful for evaluating the safety of mequindox usage in meat producing animals.

1. Introduction

Mequindox (Fig. 1), a synthetic quinoxaline 1,4-dioxides (QdNOs) derivative, was developed as a broad-spectrum antibacterial veterinary drug[1,2] and is widely used as an animal feeding additive in China.[3,4] The pharmacokinetics of the drug have been studied in a variety of species, *e.g.* rabbit,[5] sheep,[6] goat,[7] swine,[8] chicken[1] and rat.[2] Though mequindox was considered to be less harmful than other QdNOs derivatives,[9] safety concerns have been raised over the toxicity, largely regarding cellular deoxyribonucleic acid (DNA) damage.[10] Studies showed that long-term exposure to high dosages of mequindox is toxic to a rat's liver,[9,11] adrenal glands,[9,12,13] kidneys,[13] spleen[11] and testes.[14] This toxicity is mainly caused by reactive oxygen species (ROS) production during the mequindox metabolism[10,12,15] including N → O group

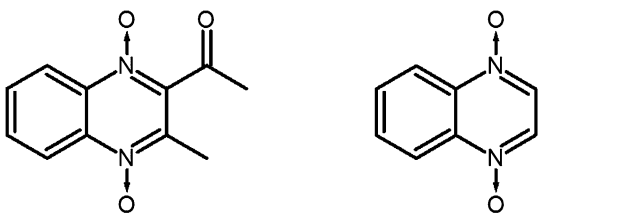

Fig. 1 Chemical structures of mequindox and quinoxaline 1,4-dioxides (QdNOs).

[a] *CAS Key Laboratory of Magnetic Resonance in Biological Systems, State Key Laboratory of Magnetic Resonance and Atomic and Molecular Physics, Wuhan Centre for Magnetic Resonance, Wuhan Institute of Physics and Mathematics, Chinese Academy of Sciences, Wuhan, 430071, P. R. China. E-mail: yulan.wang@wipm.ac.cn; Fax: +86-27-87199291; Tel: +86-27-87197143*

[b] *State Key Laboratory of Genetic Engineering, Biospectroscopy and Metabolomics, School of Life Sciences, Fudan University, Shanghai, 200433, P. R. China*

[c] *Collaborative Innovation Center for Diagnosis and Treatment of Infectious Diseases, Zhejiang University, 866 Yuhangtang Road, Hangzhou, 310058, P. R. China*

† Electronic supplementary information (ESI) available. See DOI: 10.1039/c4mb00218k

‡ Present address: Department of Diagnostic Radiology, Yong Loo Lin School of Medicine, National University of Singapore, Singapore.

§ Present address: School of Biology and Pharmaceutical Engineering, Wuhan Polytechnic University, P. R. China.

reduction, carbonyl group reduction, methyl group hydroxylation, acetyl group hydroxylation, and deacetylation.[3,4,16,17] These studies on the toxicity of mequindox were mainly carried out using targeted approaches. Recently, a holistic NMR-based metabonomics approach was employed to reveal the metabolic responses of both mice[18] and rats[19] to acute mequindox exposure. It was shown that acute high-dose mequindox exposure resulted in energy metabolism alteration, oxidative stress, liver dysfunction and gut microbial disturbance in both mice and rats. These studies have shown that NMR-based metabonomics is a very appropriate approach to characterize the metabolic responses induced by drugs.

A metabonomics study involves quantitatively detecting metabolites using NMR or mass spectrometry from biofluids or biological tissues. The high density data generated are analyzed with the aid of multivariate data analysis tools, such as Principal Component Analysis (PCA),[20] Projection to Latent Structure Discriminant Analysis (PLS-DA)[21] and Orthogonal Projection to Latent Structure Discriminant Analysis (OPLS-DA).[22] Since the birth of metabonomics, these techniques have been applied to a broad range of studies, *e.g.* disease development[23,24] and drug toxicity.[25,26]

However, the previous metabonomics investigations of mequindox[18,19] were acute studies, where the mequindox exposure periods were short (*i.e.* one week) and the drug was fed *via* gavage. If a relatively longer exposure period was employed and the drug was fed *via* a normal diet, the metabolic effect of mequindox on rodents should largely resemble the real scenario in a poultry farm. Hence, in the present study we characterized the subchronic diet-originated mequindox exposure on the system dynamic metabolic profiling of rats. NMR spectroscopy in conjunction with multivariate data analysis was used to demonstrate the metabonome alterations in urine, plasma and liver tissue extracts of rats subchronically exposed to mequindox administered at three different dose levels. Serum clinical chemistry analysis was performed to provide complementary information. The present study was aimed at providing important metabolic information on the effect of subchronic exposure to mequindox on rats, which will be useful for the safety assessment of mequindox.

2. Methods

2.1 Chemicals

Mequindox (purity 98%)[9] was provided by Prof Zonghui Yuan (Huazhong Agriculture University, Wuhan, China). Analytical grade methanol, NaCl, $K_2HPO_4{\cdot}3H_2O$ and $NaH_2PO_4{\cdot}2H_2O$ were purchased from Sinopharm Chemical Reagent Co., Ltd. (Shanghai, China). Analytical grade sodium azide (NaN_3) was obtained from Tianjin Fuchen chemical reagents factory (Tianjin, China). Deuterium oxide (D_2O, 99.9% D) and sodium 3-trimethylsilyl [2,2,3,3-$^2H_4$]-propionate (TSP) were purchased from Cambridge Isotope Laboratories, Inc. (MA, USA). Isoflurane was purchased from Shanghai Abbott Pharmaceutical Co., Ltd. (Shanghai, China).

Three different phosphate buffers were made for the preparation of urine, plasma, and liver tissue extract samples for NMR analysis. For urine samples, the phosphate buffer was prepared by dissolving K_2HPO_4 and NaH_2PO_4 in D_2O (1.5 M, pH $\approx$ 7.40, K_2HPO_4/NaH_2PO_4 = 4 : 1) containing 0.05% TSP and 0.1% NaN_3.[27] For plasma samples, the saline buffer was prepared by dissolving K_2HPO_4 and NaH_2PO_4 in water (45 mM, pH $\approx$ 7.40, K_2HPO_4/NaH_2PO_4 = 4 : 1) containing 0.9% NaCl and 50% D_2O.[19] The phosphate buffer for liver tissue extract samples was prepared by dissolving K_2HPO_4 and NaH_2PO_4 in water (0.15 M, pH 7.45, K_2HPO_4/NaH_2PO_4 = 4 : 1) containing 0.001% TSP, 0.1% NaN_3 and 50% D_2O.[26]

2.2 Animal experiments and sample collection

The animal experiments were carried out in accordance with the national guidelines for animal research (Ministry of Science and Technology, PR China, 2006) and approved by the Animal Care and Use Committee of the Chinese Academy of Sciences. A total of 144 specific pathogen free (SPF) female Wistar rats (200 g, aged 6 weeks old, No. 00004602) were purchased from the Hubei Provincial Center for Disease Control and Prevention (Hubei, China) and housed in the SPF animal facility (No. 00006027) at the Wuhan Institute of Virology (Wuhan, China, SYXK (ER) 2005-0034). All animals had free access to food and water during the entire experimental period. After 2 weeks of acclimation to the standard commercial rodent diet, the rats were randomly grouped into four groups of 36 rats. One group served as a control group (C) and was fed with the standard diet. The other three groups were respectively fed with the standard diet supplemented with 40 (L), 110 (M) and 280 (H) mg of mequindox per kg diet; the choice of dosage was based on the literature.[9] The three dosed groups were continuously fed with the mequindox supplemented diet for 13 weeks before being switched to the standard diet for 2 weeks. Urine samples were collected on a weekly basis from all rats. At 5, 13 and 15 weeks post initial dose, one-third of the rats (n = 12) in each group were randomly selected and all the selected rats were sacrificed under isoflurane anesthesia. The sacrificing procedure was always conducted in the morning. All rats were made to fast overnight before sacrifice. For each rat, serum and plasma samples were collected prior to sacrifice from the retro-orbital plexus and liver tissues were collected immediately post sacrifice. Urine, plasma and liver tissue samples were immediately snap-frozen in liquid nitrogen after collection and stored at -80 °C until NMR spectroscopic analysis. Serum samples were used for clinical chemistry measurements.

2.3 Clinical chemistry measurements

Serum clinical chemistry data were obtained by standard spectrophotometric methods using an AEROSET™ multi-task clinical chemistry system (Abbott Laboratories, Abbott Park, IL, USA). The parameters measured included alanine aminotransferase (ALT), aspartate aminotransferase (AST), alkaline phosphatase (ALP), total protein (TP), albumin (ALB), creatinine (Crea), triglycerides (TG), total cholesterol (TC) and blood glucose (Glc). Significant differences between the control and mequindox-exposed groups were determined using a one-way analysis of variance (ANOVA) at the level of $p < 0.05$.

2.4 Sample preparation for NMR analysis

The preparation of urine and plasma samples for NMR analysis was carried out as previously described.[19] Urine samples were prepared by mixing 550 μL of urine with 55 μL of phosphate buffer, and a total of 550 μL of supernatant was transferred into a 5 mm NMR tube after centrifugation (14 489*g*, 10 min, and 4 °C). Plasma samples were prepared by adding 400 μL of saline buffer into a 200 μL plasma sample and after mixing and centrifugation, 550 μL of supernatant was then transferred into a 5 mm NMR tube.

Liver tissues were extracted as previously described.[26] Briefly, liver tissues were weighed (about 50 mg) and homogenized in 600 μL of pre-cooled methanol/water (2/1) using a tissue-lyzer (QIAGEN GmbH, Germany) at 20 Hz for 90 seconds. The homogenate mixture was sonicated in an ice bath for three cycles of 1 min sonication and 1 min break. The supernatant was collected and the remaining pellets were further treated again twice using the same method. Three supernatants were combined and lyophilized after the removal of methanol *in vacuo*. The powder was reconstituted into 600 μL of phosphate buffer prepared as described above. Following a final centrifugation, 500 μL of the supernatant was transferred into a 5 mm NMR tube for NMR analysis.

2.5 NMR spectroscopy

All NMR spectra were acquired at 298 K on a Bruker Avance III 600 MHz NMR spectrometer (600.13 MHz for proton frequency) equipped with an inverse cryogenic probe (Bruker Biospin, Germany). One-dimensional (1D) ^{1}H NMR spectra were acquired for all plasma and liver tissue extract samples, while for urine samples, the 1D ^{1}H NMR acquisitions and subsequent multivariate data analysis were only performed for the samples collected at 0, 2, 5, 7, 9, 11, 13 and 15 weeks post initial dose from the 48 rats sacrificed at 15 weeks post initial dose. For urine and liver extract samples, 1D ^{1}H NMR spectra were acquired using the first increment of the gradient selected NOESY pulse sequence (recycle delay–G_1–90°–t_1–90°–t_m–G_2–90°–acquisition) with water pre-saturation during both the recycle delay (2 s) and mixing time (t_m, 80 ms). For plasma samples, 1D ^{1}H NMR spectra were acquired using the Carr–Purcell–Meiboom–Gill (CPMG) pulse sequence (recycle delay–90°–(τ–180°–τ)$_n$–acquisition), where τ = 350 μs and n = 100. A total of 32 transients for urine samples and 64 transients for plasma and liver extracts were collected into 32k data points over a spectral width of 20 ppm with a 90° pulse length adjusted to about 10 μs for all samples. The 1D ^{1}H NMR spectra were acquired in a random order for all samples.

For resonance assignment purposes, a series of two-dimensional (2D) NMR spectra were acquired for selected samples and processed as described previously,[26] including ^{1}H–^{1}H Correlation Spectroscopy (COSY), ^{1}H–^{1}H Total Correlation Spectroscopy (TOCSY), ^{1}H J-Resolved Spectroscopy (JRES), ^{1}H–^{13}C Heteronuclear Single Quantum Correlation Spectroscopy (HSQC) and ^{1}H–^{13}C Heteronuclear Multiple Bond Correlation Spectroscopy (HMBC).

2.6 NMR data processing and multivariate data analysis

All free induction decays (FIDs) were multiplied by an exponential function with a line broadening factor of 1 Hz. Prior to Fourier transformation (FT), the FIDs of urine and liver tissues were zero-filled to 128k data points, whilst the FIDs of plasma were zero-filled to 64k data points. All NMR spectra were phase- and baseline-corrected manually using Topspin (V2.0, Bruker Biospin, Germany). The spectra of urine and liver tissues were referenced to TSP (δ 0.00), whilst the spectra of plasma were referenced to the anomeric proton of α-glucose (δ 5.23). The spectral regions δ 0.50–9.65 for liver extracts, δ 0.50–10.00 for urine, and δ 0.50–8.50 for plasma were segmented into discrete bins (0.004 ppm each in width) using the AMIX software package (V3.9.5, Bruker Biospin, Germany). Regions distorted by imperfect water suppression (δ 4.46–5.16 for plasma spectra, δ 4.50–5.30 for urine spectra, and δ 4.60–5.18 for liver extract spectra) and regions containing urea signals (δ 5.40–6.00 for plasma spectra and δ 5.50–6.25 for urine spectra) were discarded. The integral areas of the remaining bins were normalized to the total sum of spectra of plasma and spectra of urine to compensate for the overall concentration differences prior to subsequent data analysis and the spectra of liver extracts were normalized to liver weights.[28]

The normalized NMR data were imported into SIMCA-P$^+$ (V11.0 and 12.0, Umetrics AB, Umea, Sweden) for multivariate data analysis. PCA was performed on the unit-variance scaled data for an overview of data distribution and the detection of possible outliers. PLS-DA and OPLS-DA were then performed on the same data using the class information as the Y-matrix. Two PLS components were calculated for PLS-DA models and one PLS and one orthogonal component were calculated for OPLS-DA models and they were all validated using a 7-fold cross-validation method.[22] Additionally, PLS models were further assessed by a permutation test with 200 permutations[29] and the OPLS-DA models with ANOVA of the cross-validated residual (CV-ANOVA) tests,[30] at the level of $p < 0.05$.

The interpretation of the OPLS-DA models was aided by back-transformed loadings incorporated with color coded correlation coefficient loading plots (MATLAB 7.0, the Mathworks Inc., Natwick, U.S.A.).[31] In these loading plots, the important metabolites contributing to the class differentiation were indicated by red color. The cutoff values for correlation coefficients were chosen based on the discrimination significance ($p < 0.05$) and in this study, a cutoff value of ($|r|$) = 0.553 was used for the sample number (n) = 12. The dynamic alterations of all important metabolites were summarized in heat maps, where the red color indicated a marked increase of metabolites in the treated groups as compared to controls, whilst the blue color indicated a marked decrease.

3. Results

3.1 Body weight changes

Compared to the control group, there was no significant difference of rat body weight within the low-dose group and a significant decrease of rat body weight within the moderate-dose and

high-dose groups at all the time points post initial dose (Table S1, ESI†). There was no significant difference of rat body weight between the moderate-dose and high-dose groups at all the time points post initial dose (Table S1, ESI†).

3.2 Clinical chemistry

Compared to the control group, there was a significant decrease of Crea and TG in serum within the low-dose group, a significant increase of TP and ALB in serum within the moderate-dose group, and a significant increase of ALB in serum within the high-dose groups, all at 5 weeks post initial dosage (Table S2, ESI†). At 13 weeks post initial dosage, there was a significant increase of AST in serum of the low-dose group, a significant increase of TP and ALB in serum of the moderate-dose group, and a significant increase of ALB and decrease of TG in serum of the high-dose group (Table S2, ESI†). At 15 weeks post initial

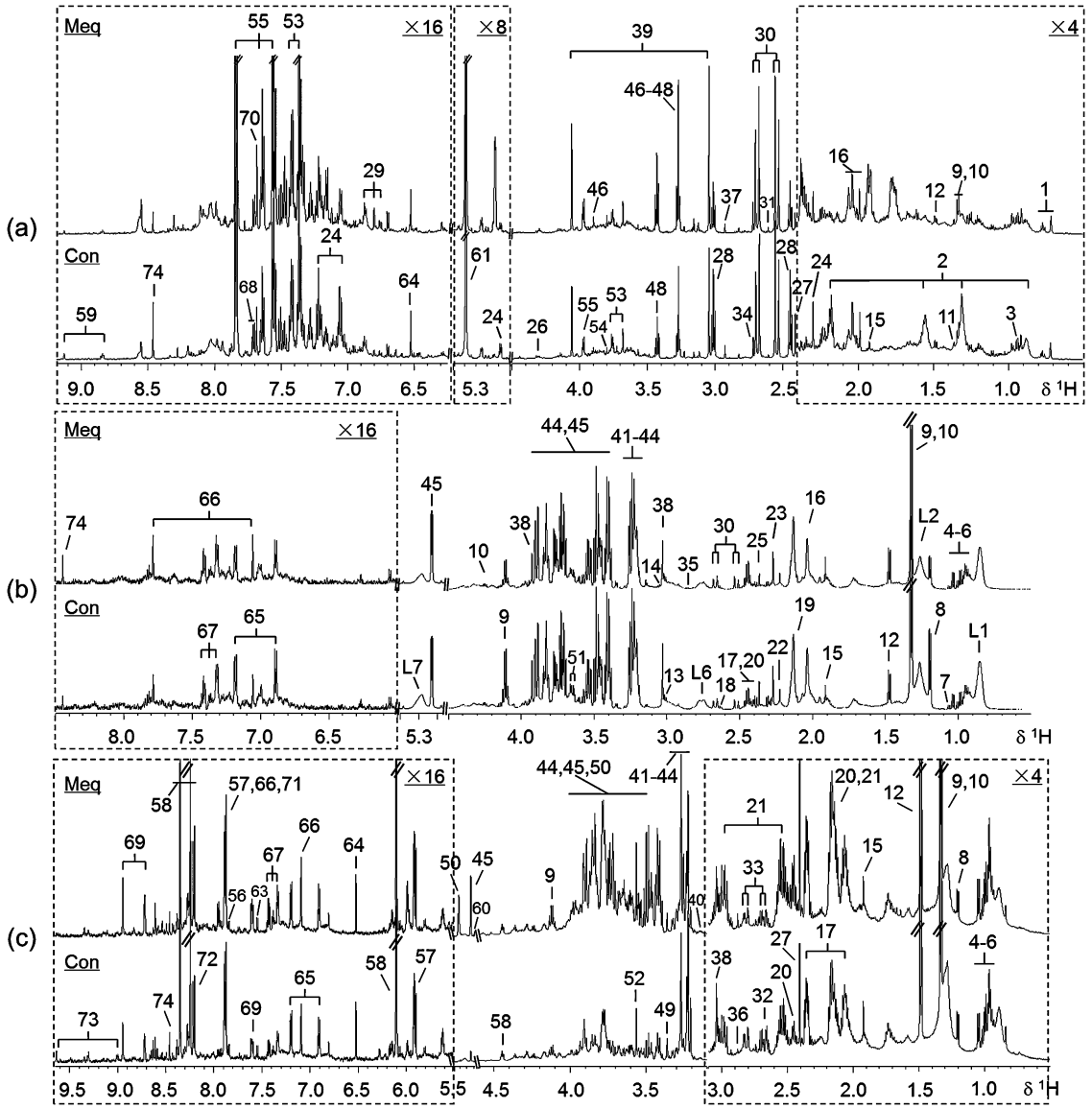

Fig. 2 600 MHz ^{1}H NMR spectra of (a) urine, (b) plasma and (c) liver tissue extracts from control (Con) and high-dose mequindox (Meq) treated rats 13 weeks post initial dose. The dotted regions were vertically expanded 16, 8 and 4 times in the spectra of a, 16 times in the spectra of b, and 16 and 4 times in the spectra of c. Metabolite keys: L1, L2, L6, L7, lipid; 1, bile acids; 2, octanoate; 3, isovalerylglycine; 4, isoleucine; 5, leucine; 6, valine; 7, dihydrothymine; 8, 3-D-hydroxybutyrate; 9, lactate; 10, threonine; 11, α-hydroxyisobutyrate; 12, alanine; 13, lysine; 14, ornithine; 15, acetate; 16, *N*-acetyl glycoproteins; 17, glutamate; 18, methionine; 19, *O*-acetyl glycoprotein; 20, glutamine; 21, oxidized glutathione; 22, acetone; 23, acetoacetate; 24, *p*-cresol glucuronide; 25, pyruvate; 26, malate; 27, succinate; 28, 2-oxoglutarate; 29, 3-(3-hydroxyphenyl)propionate; 30, citrate; 31, methylamine; 32, hypotaurine; 33, aspartate; 34, dimethylamine; 35, asparagine; 36, trimethylamine; 37, *N*,*N*-dimethylglycine; 38, creatine; 39, creatinine; 40, ethanolamine; 41, choline; 42, phosphocholine; 43, glycerophosphocholine; 44, β-glucose; 45, α-glucose; 46, betaine; 47, trimethylamine *N*-oxide; 48, taurine; 49, methanol; 50, glycogen; 51, glycerol; 52, glycine; 53, phenylacetylglycine; 54, guanidoacetate; 55, hippurate; 56, cytidine; 57, uridine; 58, adenosine; 59, 1-methylnicotinate; 60, mannose; 61, allantoin; 63, uracil; 64, fumarate; 65, tyrosine; 66, histidine; 67, phenylalanine; 68, indoxyl sulphate; 69, nicotinamide; 70, pseudouridine; 71, xanthine; 72, hypoxanthine; 73, nicotinamide mononucleotide; and 74, formate.

dosage (*i.e.* 2 weeks after stopping mequindox treatment), there was a significant decrease of TG and increase of Glc in serum within all mequindox treated groups, accompanied by a significant increase of ALP and TP in serum of the high-dose group (Table S2, ESI†).

3.3 NMR spectra of urine, plasma, and liver extracts

In the present study, a total of 34, 42 and 52 metabolites were assigned in ^{1}H NMR spectra of urine, plasma and liver extracts, respectively (Table S3, ESI†), according to the literature reports[32,33] with confirmation from 2D NMR experiments. The signals from mequindox were not detected in all samples. Typical ^{1}H NMR spectra of urine, plasma, and liver extracts from one control and one high-dose mequindox-treated rat at 13 weeks post initial dosage are shown in Fig. 2. Urinary NMR spectra of rats contain signals mainly from organic acids (*e.g.* TCA cycle intermediates), organic bases (*e.g.*, methylamine and dimethylamine), and host-gut microbial co-metabolites (*e.g.*, hippurate, phenylacetylglycine, and 3-(3-hydroxyphenyl)propionate) (Fig. 2a). The signals in NMR spectra of rat plasma are mainly from lipoproteins, a variety of amino acids, carbohydrates (*e.g.*, glucose) and organic acids (*e.g.*, lactate and 3-hydroxybutyrate) (Fig. 2b). The dominant metabolites detected in rat liver extracts include amino acids and their derivatives (*e.g.*, glutamine, glycine, and oxidized glutathione), carbohydrates (*e.g.*, glucose and glycogen), and nucleotide metabolites (*e.g.* adenosine and uridine) (Fig. 2c).

3.4 Mequindox-induced dynamic metabolic changes

The PCA was performed for all the collected urinary metabolic profiles. The PCA trajectory plot (Fig. 3) clearly shows time and dose dependent metabolic alterations induced by mequindox treatment. The urinary profiles of dosed groups deviate from the control group in the second principal component (PC), with larger deviations present in the high dose group than the low dose group. After two weeks of a diet without mequindox supplementation, the profiles of all the dosed groups appear to cluster with the control group (Fig. 3).

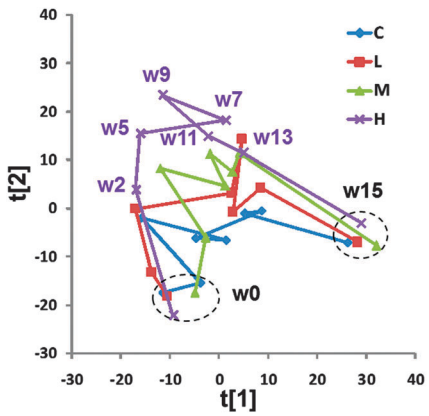

Fig. 3 A PCA trajectory plot of urinary metabolic profiles acquired for rats from the control group and three mequindox treated groups during the experimental period. Keys: C, control group; L, low-dose group; M, mid-dose group; and H, high-dose group. Time: w0, w2, w5, w7, w9, w11, and w13: 0, 2, 5, 7, 9, 11, and 13 weeks post initial dosage; w15, 2 weeks after the ceasing of mequindox treatment.

PLS-DA and OPLS-DA were subsequently performed for the profiles of urine, plasma and liver extracts, and examples of cross validated score plots and corresponding color coded coefficient plots obtained from OPLS-DA of profiles at 13 weeks post initial dose are displayed in Fig. 4. The resonance peaks pointing upwards with a red color indicate increased levels of metabolites in the dosed group and downwards peaks with a red color indicate a decrease. The parameters indicating the quality of the models (R^2 and Q^2) and the values indicating validity of the models ($p < 0.05$) obtained from the permutation test and CV-ANOVA are listed in Table S4 (ESI†). Based on the results of rigorous validation, all models constructed for profiles of urine samples are valid for the entire dose groups at all time points except at week 15, when mequindox supplementation had been stopped for two weeks. High and moderate levels of mequindox exposure induce variations in the metabolic profiles of plasma and liver, whereas no such effect is noted for the low dose group. The returning of metabolic profiles to the control level is achieved for the liver after two weeks of the washout period; however, such returning is not made for the profiles of plasma obtained from the high dose group.

The dose and time dependent alterations of metabolites for urine, plasma and liver are summarized in heat maps (Fig. 5). Urinary metabolic profiles were altered from two weeks of supplementation of mequindox. The changes of metabolite levels in the three dosed groups are broadly similar and are more prominent and persistent in the moderate and high dosed groups than in the low-dose group (Fig. 5). The alterations include marked elevation of TCA cycle intermediates (*e.g.* citrate, fumarate, malate and 2-oxoglutarate), accompanied by a noticeable decrease in the levels of urinary octanoate, isovalerylglycine, and α-hydroxyisobutyrate. In addition, alterations of a range of host-gut microbial co-metabolites were also observed. In the urine of mequindox-treated rats, there were reduced levels of *p*-cresol glucuronide, phenylacetylglycine, and methylamine, and concurrently elevated levels of hippurate and 3-(3-hydroxyphenyl)propionate. In plasma, mequindox treatment induced elevation of a range of amino acids, and resulted in a decrease in the levels of lipoprotein lipids, poly-unsaturated lipids, 3-hydroxybutyrate, acetoacetate and betaine (Fig. 5). Mequindox treatment also caused disturbances in liver; these include elevated levels of glutamine, taurine, oxidized glutathione, lactate, mannose, glucose, glycogen, uridine and nicotinamide and depletions of bile acid, 3-hydroxybutyrate, hypotaurine, choline, hypoxanthine and nicotinamide mononucleotide (Fig. 5).

4. Discussion

Despite the wide use of mequindox as a veterinary medication and an animal feeding additive,[3] the biochemical changes induced by the exposure to mequindox have not been fully investigated. Previously, the metabolic alterations induced by acute mequindox treatment (*via* gavage) in both mice[18] and rats[19] were characterized using NMR based metabonomic approaches.

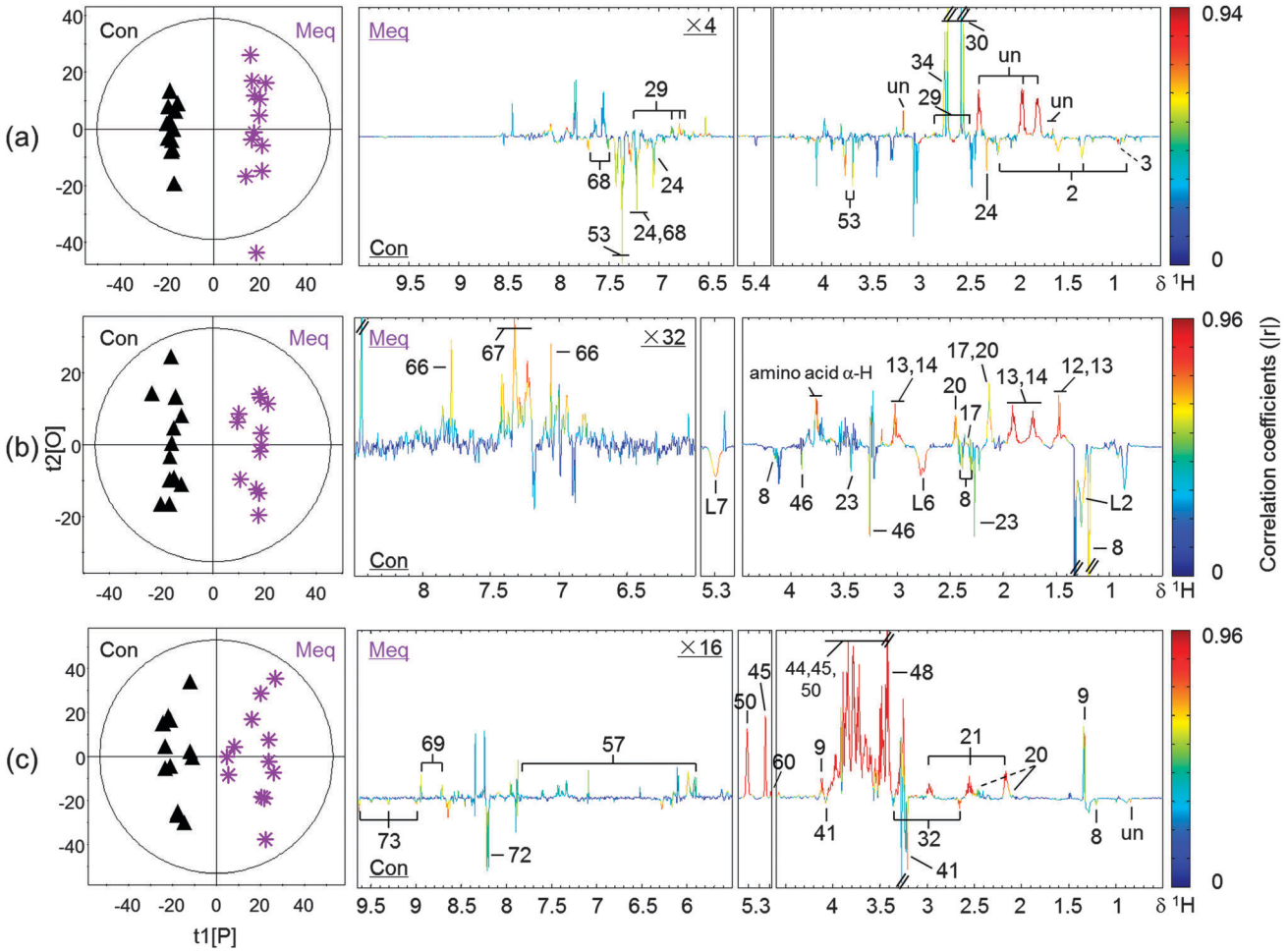

Fig. 4 Cross-validated OPLS-DA score plots (left) and the corresponding loading plots (right) derived from ^{1}H NMR spectra of (a) urine, (b) plasma and (c) liver tissue extracts for control (Con, ▲) and the high-dose mequindox treated rats (Meq, ✳) at 13 weeks post initial dose. un: undetermined metabolite; other metabolite keys are shown in Fig. 2 and Table S3 (ESI†).

The focus of the current study was to investigate the dose-dependent dynamic metabolic effect of subchronic diet-originated mequindox exposure on rats; hence we investigated the metabolic profile alterations in urine, plasma and liver tissues from rats exposed to mequindox for 13 weeks. Our investigation showed that subchronic mequindox exposure resulted in significant changes in urinary metabonome for all three dose levels starting from two weeks of the exposure (Fig. 5) and the urinary metabolic profiles returned to the control level after two weeks of the washout period. In addition, subchronic mequindox exposure at moderate and high levels also induced prominent metabolic alterations in plasma and liver, which mostly returned to the control level after two weeks of the washout period, with the exception of the profiles of plasma from high dosed rats. At the molecular level, subchronic exposure of rats to mequindox caused alterations in energy metabolism, resulted in oxidative stress, and disturbed host gut microbial co-metabolism (Fig. 6).

The prominent metabolic changes induced by mequindox exposure were the elevation of TCA cycle intermediates, including citrate, fumarate, malate and 2-oxoglutarate, in the urine and fumarate in the liver samples from rats exposed to mequindox. This observation is consistent with the acute response of mice to mequindox[18] and it indicates that the TCA cycle was stimulated in rats subchronically exposed to mequindox. However, this rise in energy circulation appeared not to come from glycolysis since we observed marked accumulation of glucose and glycogen in the liver of treated rats. Meanwhile some gluconeogenic amino acids, including alanine, glutamate, glutamine, methionine, histidine and phenylalanine, were up-regulated in exposed rats. It may imply the depressed glycolysis and promoted gluconeogenesis in rats induced by subchronic mequindox exposure. The other possible energy source would be oxidation of lipids. Indeed, the concentrations of plasma lipids, including both unsaturated and polyunsaturated lipids, were attenuated after mequindox treatment, which is also in accordance with the previous studies.[18,19] This would also explain the down-regulated serum TG levels in rats exposed to mequindox as observed in serum clinical chemistry. Taking all these results together, we conclude that lipid oxidation might act as an alternate source for energy production in rats subchronically exposed to mequindox for a long period of time. This notion is in agreement with the previous study on mice exposed acutely to high levels of mequindox.[18] Fatty acids are

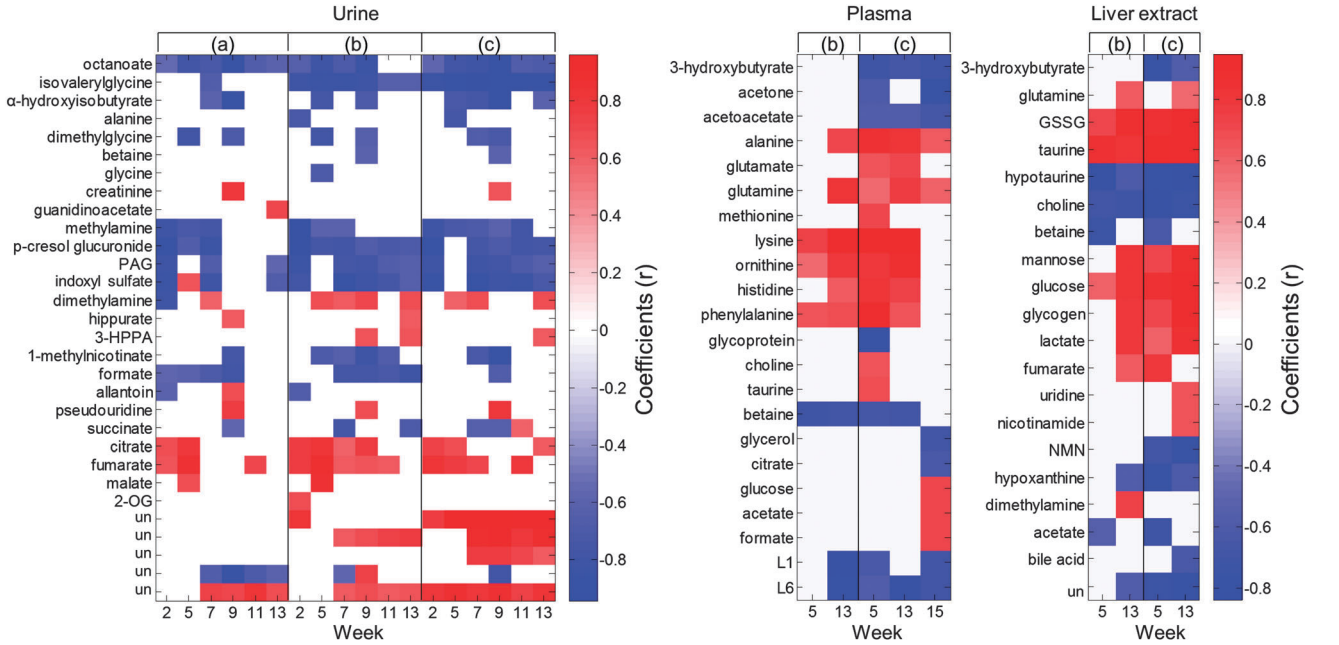

Fig. 5 Dynamic alterations of the metabolic profiles in rat urine (left), plasma (middle) and liver extracts (right) in response to different dosages of mequindox treatment. Key: a, low-dose group; b, moderate-dose group; and c, high-dose group. Abbreviations: PAG, phenylacetylglycine; 3-HPPA, 3-(3-hydroxyphenyl)propionate; 2-OG, 2-oxoglutarate; L1, L6, lipid; GSSG, glutathione disulfide; NMN, nicotinamide mononucleotide; and un: undetermined metabolite.

broken down to acetoacetyl-CoA and then acetyl-CoA, which enters the TCA cycle for energy production.[34] During the breakdown of fatty acids, ketone bodies are produced as by-products. However, the levels of ketone bodies were down-regulated after mequindox exposure in the present study, *i.e.* the decreases in the levels of D-3-hydroxybutyrate, acetone and acetoacetate were observed in rat plasma, and the decreases in the levels of D-3-hydroxybutyrate were also detected in the rat liver. It seems that the produced ketone bodies were reconverted to acetyl-CoA, which subsequently entered the TCA cycle for further energy production.[34]

When lipid oxidation acted as the main source for energy production, ROS would be formed. In addition, the *N*-oxide reductive metabolism of mequindox could also lead to the increase of intracellular ROS.[3,15] ROS formation would ultimately lead to oxidative stress in rats.[11,14] Hepatic glutathione (GSH) has a variety of physiological functions, including protection against oxidative damage and detoxification of exogenous and endogenous compounds.[35] During the anti-oxidative process, GSH is catalyzed by glutathione peroxidase to form glutathione disulfide (GSSG), resulting in the decrease of intracellular GSH and the GSH/GSSG ratio.[36] Here, increased liver GSSG levels were observed in rats exposed to moderate and high levels of mequindox at both 5 and 13 weeks post initial dose, which suggested that subchronic mequindox exposure activated anti-oxidative activity in rats. The decrease of plasma poly-unsaturated lipid levels in mequindox treated rats probably also resulted from such induced oxidative stress. In addition, we also observed altered levels of hypotaurine and taurine in the liver of rats treated with a high dose of mequindox. Both of the metabolites anticipated anti-oxidative processes, concurrent with previous reports showing that hypotaurine acts as an antioxidant *in vivo* and is oxidized to taurine under oxidative stress.[37] Furthermore, the depletion of hypoxanthine in the liver of rats exposed to a high dose of mequindox is also associated with oxidative stress, since hypoxanthine could be oxidized to xanthine and uric acid by the catalytic action of xanthine oxidase (XO) during oxidative stress.[38] In accordance with activation of anti-oxidative activity of rats, we also observed the promotion of the vitamin B3 anti-oxidative cycle[19] in the rats exposed to mequindox, which is manifested in the marked decrease in the levels of urinary 1-methylnicotinate and altered levels of nicotinamide and nicotinamide mononucleotide in the rat liver.

Mequindox is an antibiotic drug; the disruption of gut microbiota is anticipated to be associated with subchronic mequindox exposure. The disruption of gut microbiota can be reflected by alterations of mammalian-microbial co-metabolites.[39] For example, hippurate is formed by conjugation of glycine with benzoate in the liver of mammals,[40] whilst benzoate is mainly derived from aromatic acids or plant phenolics by the action of intestinal microflora.[41] Reduction in the level of urinary hippurate has been previously observed in rodents after treatment with antibiotics, such as cephaloridine,[42,43] vancomycin[44] and penicillin in combination with streptomycin sulfate.[45] Similar to hippurate, phenylacetylglycine is formed in the liver by conjugation of glycine with phenylacetate, which arose from anaerobic bacterial metabolism of phenylalanine and phenols.[45] In addition, urinary *p*-cresol glucuronide and 3-(3-hydroxyphenyl)propionate were shown to be gut microbial products of tyrosine.[46–48] Alterations of these metabolites in mequindox exposed rats suggested that mequindox exposure resulted in a disturbance of intestinal microbial colonies in rats. Another metabolic pathway affected by gut

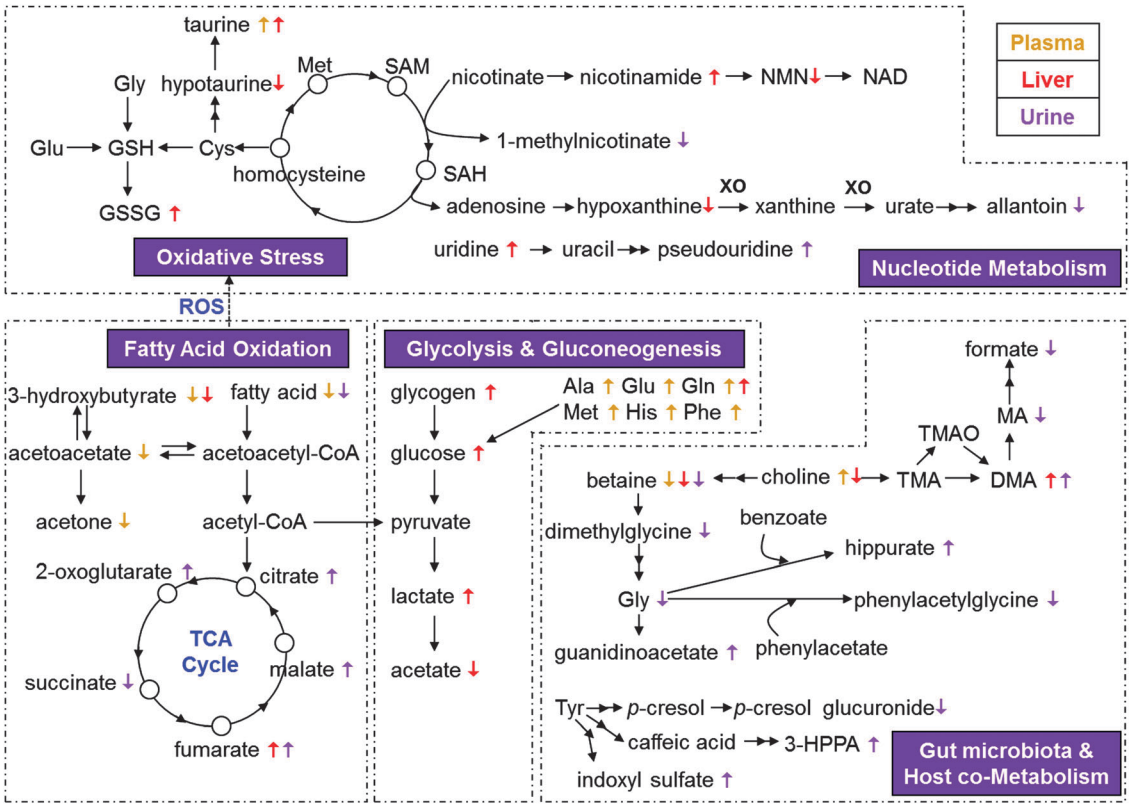

Fig. 6 Subchronic exposure to mequindox induced metabolic profile alterations in rat urine, plasma and liver tissue. Symbols: colored up arrows (↑) indicate the increase of metabolite levels in mequindox treated rats compared to controls, while colored down arrows (↓) indicate the decrease. Arrow colors: brown, red, and purple colors indicate that alterations of metabolite concentration occurred in rat plasma, liver and urine respectively. Abbreviations: NAD, nicotinamide adenine dinucleotide; NMN, nicotinamide mononucleotide; SAM, *S*-adenosyl-L-methionine; SAH, *S*-adenosyl-L-homocysteine; GSH, glutathione; GSSG, glutathione disulfide; XO, xanthine oxidase; CoA, Coenzyme A; TCA, tricarboxylic acid; 3-HPPA, 3-(3-hydroxyphenyl)propionate; MA, methylamine; DMA, dimethylamine; TMA, trimethylamine; TMAO, trimethylamine *N*-oxide; ROS, reactive oxygen species; and other three letter abbreviations are standard amino acid abbreviations.

microbiota is choline metabolism. Choline can be metabolized by host-microbial interactions, resulting in the formation of amines.[49,50] Here we observed the decreased levels of choline in the liver with concomitant increased levels of dimethylamine in the liver and urine, and decreased levels of urinary methylamine and formate in the rats exposed to mequindox. The gut microbial associated alteration of choline metabolism also affected the conversion of choline into other metabolites, through stepwise enzymatic reactions, such as betaine, dimethylglycine, glycine, guanidinoacetate and creatinine (Fig. 6). The disturbances of host-gut microbial co-metabolism may have some effect on nutrient uptake from diet and hence the growth of rats.

5. Conclusion

The current study clearly shows that subchronic diet-originated low dose (40 mg kg^{-1}) mequindox exposure only affects rat urinary metabonome, while moderate dose (110 mg kg^{-1}) and high dose (280 mg kg^{-1}) mequindox exposure induced significant alterations in the metabonomes of urine, liver and plasma. Metabolic alterations during mequindox supplementation in rats include a stimulated TCA cycle, suppression of glycolysis, promotion of gluconeogenesis and lipid oxidation, induced oxidative stresses and disturbances of host-gut microbial co-metabolism. The present study also demonstrated that NMR-based metabonomics is very suitable for monitoring the system dynamic metabolic effects of subchronic exposure to mequindox on rats, which is useful for assessing the safety of mequindox and other veterinary drugs used in farm animals.

Acknowledgements

We acknowledge the financial support from the Ministry of Science and Technology of China (2009CB118804, 2012CB934004, 2011YQ12003503) and National Natural Science Foundation of China (20921004).

References

1 H. Z. Ding, Y. C. Liu, Z. L. Zeng, H. B. Si, K. Y. Liu, Y. M. Liu, F. Yang, Y. F. Li and D. P. Zeng, *Res. Vet. Sci.*, 2012, **93**, 374–377.
2 G. H. Li, F. Yang, L. M. He, H. Z. Ding, N. Sun, Y. C. Liu, Y. M. Liu, Q. Shan, Y. F. Li and Z. L. Zeng, *Res. Vet. Sci.*, 2012, **93**, 1380–1386.

3 X. Q. Tang, P. Q. Mu, J. Wu, J. Jiang, C. H. Zhang, M. Zheng and Y. Q. Deng, *Drug Metab. Dispos.*, 2012, **40**, 788–795.
4 J. Liu, X. H. Ge, O. Y. Man, X. Q. Tang, J. Wu, J. P. Wang, J. Jiang, M. S. Y. Huen and Y. Q. Deng, *Catal. Commun.*, 2011, **12**, 637–643.
5 C. W. Lu, Y. Q. Li, Y. J. Guan, Y. B. Zhang, D. Y. Bai, X. L. Miao and Y. J. Xiong, *Journal of Northwest A & F University (Nat. Sci. Ed.)*, 2008, **36**, 29–34.
6 Y. Q. Huang, Y. Q. Li, Y. J. Yang, X. L. Miao, Y. Xie, D. Y. Bai, C. W. Lu, L. Sun and B. Z. Ma, *Journal of Northwest A & F University (Nat. Sci. Ed.)*, 2008, **36**, 77–81.
7 Y. Q. Li, W. Y. Xie, X. Y. Zhang, Z. H. Tian and C. J. Hao, *Afr. J. Biotechnol.*, 2010, **9**, 8472–8476.
8 Y. M. Liu, Y. C. Liu, H. Z. Ding, B. H. Fang, F. Yang, Q. Shan and Z. L. Zeng, *Agric. Sci. China*, 2011, **10**, 1968–1976.
9 A. Ihsan, X. Wang, X. J. Huang, Y. Liu, Q. Liu, W. Zhou and Z. H. Yuan, *Regul. Toxicol. Pharmacol.*, 2010, **57**, 307–314.
10 J. Liu, M. Ouyang, J. Jiang, P. Q. Mu, J. Wu, Q. Yang, C. H. Zhang, W. Y. Xu, L. J. Wang, M. S. Y. Huen and Y. Q. Deng, *Mutat. Res., Genet. Toxicol. Environ. Mutagen.*, 2012, **741**, 70–75.
11 X. Wang, X. J. Huang, A. Ihsan, Z. Y. Liu, L. L. Huang, H. H. Zhang, H. F. Zhang, W. Zhou, Q. Liu, X. J. Xue and Z. H. Yuan, *Toxicology*, 2011, **280**, 126–134.
12 X. J. Huang, A. Ihsan, X. Wang, M. H. Dai, Y. L. Wang, S. J. Su, X. J. Xue and Z. H. Yuan, *Toxicol. Lett.*, 2009, **191**, 167–173.
13 X. J. Huang, X. Wang, A. Ihsan, Q. Liu, X. J. Xue, S. J. Su, C. H. Yang, W. Zhou and Z. H. Yuan, *Toxicol. Lett.*, 2010, **198**, 112–118.
14 A. Ihsan, X. Wang, Z. Y. Liu, Y. L. Wang, X. J. Huang, Y. Liu, H. Yu, H. F. Zhang, T. T. Li, C. H. Yang and Z. H. Yuan, *Toxicol. Appl. Pharmacol.*, 2011, **252**, 281–288.
15 X. J. Huang, H. H. Zhang, X. Wang, L. L. Huang, L. Y. Zhang, C. X. Yan, Y. Liu and Z. H. Yuan, *Chem.-Biol. Interact.*, 2010, **185**, 227–234.
16 Z. Y. Liu, L. L. Huang, D. M. Chen and Z. H. Yuan, *Rapid Commun. Mass Spectrom.*, 2010, **24**, 909–918.
17 Q. Shan, Y. M. Liu, L. M. He, H. Z. Ding, X. H. Huang, F. Yang, Y. F. Li and Z. L. Zeng, *J. Chromatogr. B: Anal. Technol. Biomed. Life Sci.*, 2012, **881–882**, 96–106.
18 X. J. Zhao, C. Y. Huang, H. H. Lei, X. Nie, H. R. Tang and Y. L. Wang, *J. Proteome Res.*, 2011, **10**, 5183–5190.
19 X. J. Zhao, F. H. Hao, C. Y. Huang, M. Rantalainen, H. H. Lei, H. R. Tang and Y. L. Wang, *J. Proteome Res.*, 2012, **11**, 4712–4721.
20 J. C. Lindon, E. Holmes and J. K. Nicholson, *Prog. Nucl. Magn. Reson. Spectrosc.*, 2001, **39**, 1–40.
21 J. Trygg, E. Holmes and T. Lundstedt, *J. Proteome Res.*, 2007, **6**, 469–479.
22 J. Trygg and S. Wold, *J. Chemom.*, 2002, **16**, 119–128.
23 Y. L. Wang, E. Holmes, J. K. Nicholson, O. Cloarec, J. Chollet, M. Tanner, B. H. Singer and J. Utzinger, *Proc. Natl. Acad. Sci. U. S. A.*, 2004, **101**, 12676–12681.
24 Y. L. Wang, J. Utzinger, J. Saric, J. V. Li, J. Burckhardt, S. Dirnhofer, J. K. Nicholson, B. H. Singer, R. Brun and E. Holmes, *Proc. Natl. Acad. Sci. U. S. A.*, 2008, **105**, 6127–6132.
25 L. M. Zhang, Y. F. Ye, Y. P. An, Y. A. Tian, Y. L. Wang and H. R. Tang, *J. Proteome Res.*, 2011, **10**, 614–623.
26 L. M. Jiang, J. Huang, Y. L. Wang and H. R. Tang, *J. Proteome Res.*, 2012, **11**, 3848–3859.
27 C. N. Xiao, F. H. Hao, X. R. Qin, Y. L. Wang and H. R. Tang, *Analyst*, 2009, **134**, 916–925.
28 C. Y. Huang, H. H. Lei, X. J. Zhao, H. R. Tang and Y. L. Wang, *J. Proteome Res.*, 2013, **12**, 537–545.
29 F. Lindgren, B. Hansen, W. Karcher, M. Sjostrom and L. Eriksson, *J. Chemom.*, 1996, **10**, 521–532.
30 L. Eriksson, J. Trygg and S. Wold, *J. Chemom.*, 2008, **22**, 594–600.
31 O. Cloarec, M. E. Dumas, J. Trygg, A. Craig, R. H. Barton, J. C. Lindon, J. K. Nicholson and E. Holmes, *Anal. Chem.*, 2005, **77**, 517–526.
32 W. M. T. Fan, *Prog. Nucl. Magn. Reson. Spectrosc.*, 1996, **28**, 161–219.
33 H. R. Tang, Y. L. Wang, J. K. Nicholson and J. C. Lindon, *Anal. Biochem.*, 2004, **325**, 260–272.
34 A. L. Lehninger, D. L. Nelson and M. M. Cox, in *Lehninger principles of biochemistry*, ed. A. L. Lehninger and W. H. Freeman, New York, 2005, ch. 17, pp. 631–655.
35 L. D. Deleve and N. Kaplowitz, *Semin. Liver Dis.*, 1990, **10**, 251–266.
36 J. Y. Xu, Y. Y. Su, J. S. Cheng, S. X. Li, R. L. Liu, W. X. Li, G. T. Xu and Q. N. Li, *Carbon*, 2010, **48**, 1388–1396.
37 R. J. Huxtable, *Physiol. Rev.*, 1992, **72**, 101–163.
38 O. Yoshiji, K.-N. Mutsumi, I. Yoichiro and K. Teruaki, *J. Clin. Biochem. Nutr.*, 2003, **33**, 83–93.
39 B. L. Goodwin, C. R. J. Ruthven and M. Sandler, *Biochem. Pharmacol.*, 1994, **47**, 2294–2297.
40 A. N. Phipps, J. Stewart, B. Wright and I. D. Wilson, *Xenobiotica*, 1998, **28**, 527–537.
41 R. R. Scheline, *Acta Pharmacol. Toxicol.*, 1968, **26**, 189–205.
42 M. L. Anthony, K. P. R. Gartland, C. R. Beddell, J. C. Lindon and J. K. Nicholson, *Arch. Toxicol.*, 1992, **66**, 525–537.
43 L. B. Murgatroyd, R. J. Pickford, I. K. Smith, I. D. Wilson and B. J. Middleton, *Hum. Exp. Toxicol.*, 1992, **11**, 35–41.
44 I. K. S. Yap, J. V. Li, J. Saric, F. P. Martin, H. Davies, Y. L. Wang, I. D. Wilson, J. K. Nicholson, J. Utzinger, J. R. Marchesi and E. Holmes, *J. Proteome Res.*, 2008, **7**, 3718–3728.
45 J. R. Swann, K. M. Tuohy, P. Lindfors, D. T. Brown, G. R. Gibson, I. D. Wilson, J. Sidaway, J. K. Nicholson and E. Holmes, *J. Proteome Res.*, 2011, **10**, 3590–3603.
46 Y. L. Wang, J. Utzinger, S. H. Xiao, J. Xue, J. K. Nicholson, M. Tanner, B. H. Singer and E. Holmes, *Mol. Biochem. Parasitol.*, 2006, **146**, 1–9.
47 R. R. Scheline and T. Midtvedt, *Experientia*, 1970, **26**, 1068–1069.
48 A. W. Nicholls, R. J. Mortishire-Smith and J. K. Nicholson, *Chem. Res. Toxicol.*, 2003, **16**, 1395–1404.
49 J. L. Smith, J. S. Wishnok and W. M. Deen, *Toxicol. Appl. Pharmacol.*, 1994, **125**, 296–308.
50 M. E. Dumas, R. H. Barton, A. Toye, O. Cloarec, C. Blancher, A. Rothwell, J. Fearnside, R. Tatoud, V. Blanc, J. C. Lindon, S. C. Mitchell, E. Holmes, M. I. McCarthy, J. Scott, D. Gauguier and J. K. Nicholson, *Proc. Natl. Acad. Sci. U. S. A.*, 2006, **103**, 12511–12516.

